Discordant Calcium Transient and Action Potential Alternans in a Canine Left-Ventricular Myocyte

Citation: Armoundas, A.A. "Discordant Calcium Transient and Action Potential Alternans in a Canine Left-Ventricular Myocyte." Biomedical Engineering, IEEE Transactions on 56.9 (2009): 2340-2344. © 2009 Institute of Electrical and Electronics Engineers

As Published: http://dx.doi.org/10.1109/tbme.2009.2023671

Publisher: Institute of Electrical and Electronics Engineers

Persistent URL: http://hdl.handle.net/1721.1/52424

Version: Final published version: final published article, as it appeared in a journal, conference proceedings, or other formally published context

Discordant Calcium Transient and Action Potential Alternans in a Canine Left-Ventricular Myocyte

Antonis A. Armoundas, *Senior Member, IEEE*

***Abstract*—Electrocardiographic alternans is known to predispose to increased susceptibility to life threatening arrhythmias and sudden cardiac death. While this decreased level of cardiac electrical stability is often due to the presence of discordant action potential (AP) alternans in the heart, the mechanism of discordant cardiac alternans remains unknown. This study presents a case report of cellular discordant cardiac alternans between AP and $[Ca^{2+}]_i$ and employs a novel reverse engineering approach that applies a simultaneous AP and $[Ca^{2+}]_i$ clamp of experimentally obtained data to a left-ventricular canine myocyte model, to probe its underlying mechanism. The model results indicate that during alternans, the increased sarcoplasmic reticulum Ca^{2+}, triggers multiple ryanodine receptor (RyR) channel openings and delayed Ca^{2+} release, which subsequently triggers an inward depolarizing current, a subthreshold early after-depolarization, and AP prolongation. The amplitude of $[Ca^{2+}]_i$ plays a critical role in defining the concordant or discordant relationship between the $[Ca^{2+}]_i$ and AP at the myocyte level. In conclusion, the results presented in this study support the idea that aberrant RyR openings on alternate beats are responsible for the $[Ca^{2+}]_i$ alternan-type oscillations, which, in turn, give rise to an in- or out-of-phase relationship between $[Ca^{2+}]_i$ and AP alternans.**

***Index Terms*—Cellular alternans, model, myocyte, ryanodine receptor (RyR), sarcoplasmic reticulum (SR).**

I. Introduction

T-WAVE alternans has been associated with an increased risk to arrhythmias [1] and sudden cardiac death (SCD) [2], [3].

However, at the myocyte level, it is still unclear what triggers action potential (AP) alternans. It was recently shown that the morphology of the AP (through its modulation by sarcolemmal Ca^{2+} [4] and K^+ [5], [6] currents) has a significant effect on the stability of the Ca^{2+} handling processes and the transition from normal intracellular Ca^{2+} ($[Ca^{2+}]_i$) to stable $[Ca^{2+}]_i$ alternans [7]. However, other studies have suggested that $[Ca^{2+}]_i$ alternans give rise to AP alternans [7]–[15]; thus, according to this hypothesis, $[Ca^{2+}]_i$ alternans resulting from stress-induced [1], [8] deficiencies in any number of Ca^{2+} transport processes may, in turn, give rise to AP alternans. Irrespective of the proposed hypothesis, common characteristic of all studies was that the $[Ca^{2+}]_i$ and AP oscillated in phase (concordant alternans; for definitions, see Section II).

This study presents the first report of discordant (out of phase) $[Ca^{2+}]_i$ and AP alternans at the myocyte level and employs a novel hybrid experimental–computational approach to probe the mechanisms underlying the relationship between $[Ca^{2+}]_i$ and AP alternans.

Manuscript received December 14, 2008; revised February 17, 2009. First published June 2, 2009; current version published August 14, 2009. This work was supported by the American Heart Association awards under Beginning Grant-in-Aid 0365304U and under Scientist Development Grant 0635127N.

The author is with the Cardiovascular Research Center, Massachusetts General Hospital, Boston, MA 02129 USA, and also with Massachusetts Institute of Technology, Cambridge, MA 02139 USA (e-mail: aarmoundas@partners.org).

Digital Object Identifier 10.1109/TBME.2009.2023671

II. Methods

A. Definitions

Concordant and discordant alternans at the whole heart as well as the myocyte level are defined as follows.

1) *Large/small* $[Ca^{2+}]_i$ *during alternans*, refers to $[Ca^{2+}]_i$ amplitude that is larger/smaller than its immediately preceding $[Ca^{2+}]_i$.
2) *Long/short AP duration (APD) during alternans*, refers to APD that is longer/shorter than its immediately preceding APD.
3) *Concordant* APD *alternans* between two areas in the heart refer to APD oscillations that are in-phase, i.e., both areas exhibit either long or short APDs.
4) *Discordant APD alternans between two areas in the heart* refer to APD oscillations that are out-of-phase, i.e., one area exhibits long APDs, while the other exhibits short APDs.
5) *Concordant alternans between* $[Ca^{2+}]_i$ *and AP at the single myocyte* refer to oscillations of these signals that are in-phase, i.e., a large $[Ca^{2+}]_i$ corresponds to a long APD and *vice versa*.
6) *Discordant alternans between* $[Ca^{2+}]_i$ *and AP at the single myocyte* refer to oscillations of these signals that are out-of-phase, i.e., a large $[Ca^{2+}]_i$ corresponds to a short APD and *vice versa*.

B. Myocyte Isolation and Electrophysiological Studies

A canine-isolated left-ventricular myocyte [15] was whole-cell patch-clamped at 37 °C in a heated chamber on the stage of an inverted fluorescence microscope (Olympus IX70). Borosilicate glass pipettes of 3–5 MΩ tip resistance were used for whole-cell recording of APs or membrane currents with an Axopatch 200B amplifier digitized via a Digidata 1200A (Axon Instruments) personal computer interface.

A xenon arc lamp was used to excite indo-1 fluorescence at 365 nm (390 nm dichroic mirror), and the emitted fluorescence was recorded using a dual-channel photomultiplier tube assembly (ESP associates, Toronto, ON, Canada) at wavelengths of 405 and 495 nm. Cellular autofluorescence at both emission

wavelengths was recorded before rupturing the cell-attached patch. The ratio of indo-1 fluorescence ($R = \mathrm{F}_{405\,\mathrm{nm}}/\mathrm{F}_{495\,\mathrm{nm}}$) was determined after subtraction of cellular autofluorescence, and was used to calculate free intracellular Ca^{2+} according to the equation $[Ca^{2+}]_i = K_d\beta[(R - R_{\min})/(R_{\max} - R)]$, using a K_d of 844 nmol/L [16]. The $R_{\min}, R_{\max}$, and β for the fluorescence system were determined to be 0.45, 2.4, and 3.8, respectively [16]. Electrophysiological and fluorescence signals were acquired simultaneously and analyzed offline.

The myocyte was patched using physiological extracellular solution containing (in millimoles per liter): NaCl 138, KCl 4, $MgCl_2$ 1, $CaCl_2$ 2, NaH_2PO_4 0.33, glucose 10, and 4-(2-hydroxyethyl)-1-piperazineethanesulfonic acid, (HEPES) 10; pH 7.4 with NaOH, and intracellular solution containing (in millimoles per liter): potassium glutamate 130, KCl 9, NaCl 10, $MgCl_2$ 0.5, MgATP 5, and HEPES 10; pH 7.2 with KOH and 50 μmol/L indo-1 (Molecular Probes). The pipette-to-bath liquid junction potential was -17 mV, and was corrected.

The myocyte was stimulated in current clamp at progressively faster frequencies until alternans was elicited.

C. Canine Left-Ventricular Myocyte Model

A simultaneous $[Ca^{2+}]_i$- and AP-clamp variation of the canine left-ventricular myocyte computer model [15]–[18] was developed, which permitted to input experimentally obtained records of $[Ca^{2+}]_i$ and AP as a driving function, and compute, in isolation, the intracellular compartments' Ca^{2+} concentration and fluxes as well as the underlying membrane currents (i.e., the L-type current, the sodium–calcium exchanger, etc).

III. Results

A. Concordant and Discordant $[Ca^{2+}]_i$ and AP Alternans

Fig. 1(a) presents sustained concordant (in phase) $[Ca^{2+}]_i$ and AP alternans recorded from an epicardial left-ventricular myocyte stimulated every 0.8 s. After some period of sustained concordant $[Ca^{2+}]_i$ and AP alternans in the same data record, in Fig. 1(b), one notices examples of discordant $[Ca^{2+}]_i$ and AP alternans; specifically, one observes that the in-phase relationship between $[Ca^{2+}]_i$ and AP is altered at point (a) to become discordant (out-of-phase), becomes again concordant at point (b), changes to discordant at point (c), and finally, becomes concordant at (d).

To investigate the complex interplay between the sarcolemmal potential and ionic currents with the sarcoplasmic reticulum (SR) Ca^{2+} fluxes (uptake and release), a simultaneous AP- and $[Ca^{2+}]_i$-clamp approach was applied to a previously described left-ventricular canine myocyte model [16]. The model was clamped with the experimentally recorded $[Ca^{2+}]_i$ and AP data, a segment of which is presented in Fig. 1(b), and the resulting sarcolemmal ionic currents and SR Ca^{2+} fluxes are presented in Fig. 2.

Thus, in Fig. 2(a), the left axis presents the APD_{90} and the right axis presents the $\Delta[Ca^{2+}]_i$ (defined as systolic minus diastolic $[Ca^{2+}]_i$) of the beat-to-beat fluctuations of the corresponding beats in Fig. 1(b), which were used to clamp the model. In

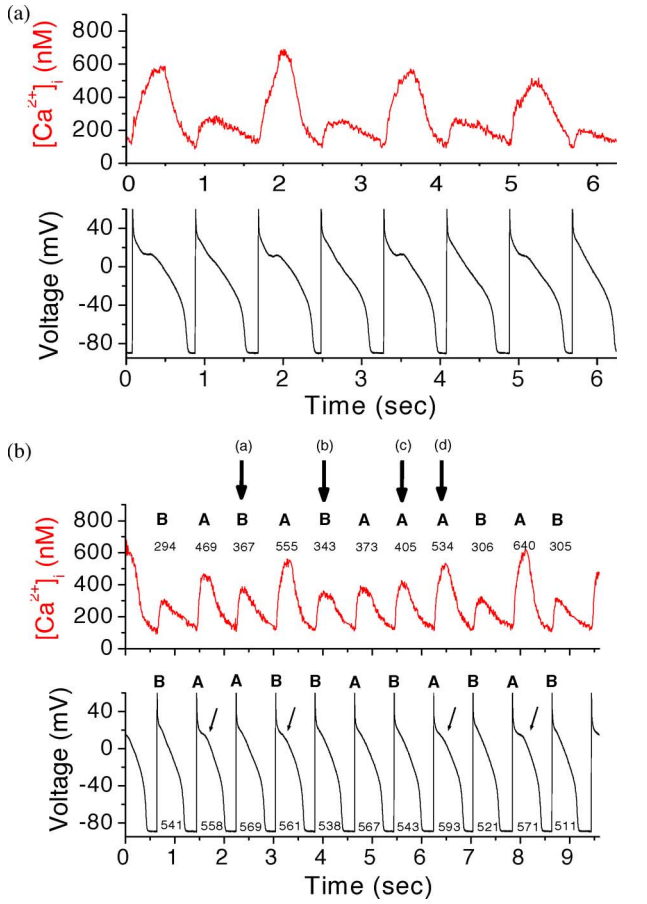

Fig. 1. (a) Representative example of concordant $[Ca^{2+}]_i$ and AP alternans in ventricular myocyte stimulated every 0.8 s; (b) representative example of phase transitions between $[Ca^{2+}]_i$ and AP alternans indicated at points (a) to (d), in the same data record. In-phase (concordant) $[Ca^{2+}]_i$ and AP alternans leads to out-of-phase (discordant) alternans indicated at points (a) and (c), and back again to in-phase alternans indicated in beats (b) and (d). "A" and "B" denote large and small $[Ca^{2+}]_i$ or long and short APD respectively; the peak $[Ca^{2+}]_i$ and APD for these beats are also shown. The arrows in the voltage tracing of (b) indicate a sub-threshold after early after-depolarization.

Fig. 2(b), the left axis presents the time-dependent beat-to-beat current attributed to both the L-type calcium channel (LTCC) ($I_{\mathrm{Ca},L}$) and the Na/Ca exchanger (I_{NCX}), while the right axis presents the ryanodine receptor (RyR) open probability of the same beats presented in Fig. 1(b); in this figure, the choice of lumping the two currents is based on the hypothesis that if $[Ca^{2+}]_i$ and AP alternans are linked, it is likely that the balance (reflected in the sum) of these two currents that control the depolarization versus repolarization of the membrane, will determine their effect on the APD.

One observes that the APD prolongation observed in Fig. 2(a) is associated with the larger inward depolarizing current attributed to the LTCC and the NCX seen in Fig. 2(b); this depolarizing current is a result of secondary, much smaller SR Ca^{2+} release events, reflected at the RyR state-1 open probability P_{O1} [see Fig. 2(b)] on an every other beat basis indicated by an "$*$," while the primary SR Ca^{2+} release events are represented by an "$\uparrow$." This depolarizing current is associated with a small deflection on the AP [also seen after careful inspection in Fig. 1(b)],

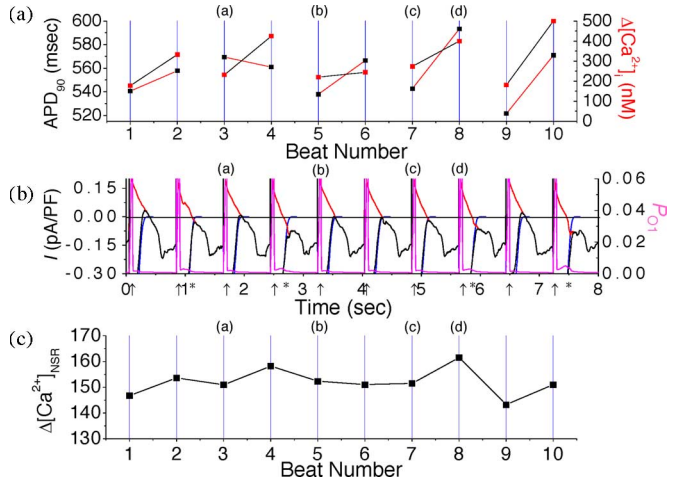

Fig. 2. $[Ca^{2+}]_i$ and AP experimental data of Fig. 1(b) were used to simultanously $[Ca^{2+}]_i$ - and voltage-clamp the canine myocyte model. (a) Left ordinate presents the beat-to-beat experimentally measured APD (in black) and the right ordinate presents $\Delta[Ca^{2+}]_i$ (expressed as systolic minus diastolic $[Ca^{2+}]_i$, and is shown in red); data are plotted in pairs to demonstrate the alternans beat-to-beat oscillations. (b) Left ordinate presents the sum (black line) of the $I_{Ca,L}$ (blue line) and I_{NCX} (red line), and the right ordinate the RyR state 1 open probability P_{O1} (magenta line). (c) the sarcoplasmic reticulum ($[Ca^{2+}]_{SR}$) is presented for the same beats in (a) and (b). (↑): indicates primary RyR openings; (∗): indicates secondary RyR openings.

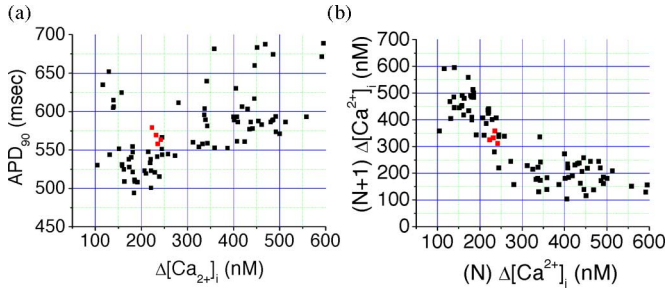

Fig. 3. Presence of phase transitions between $[Ca^{2+}]_i$ and AP (red pixels) in experimentally obtained $\Delta[Ca^{2+}]_i$ and APD time series. (a) The relationship between the APD and $\Delta[Ca^{2+}]_i$ (systolic minus diastolic $[Ca^{2+}]_i$), which indicates that phase reversal occurs when the APD falls within a small range of its minimum and maximum values ($113\% \leq APD_{rev}/APD_{min} \leq 117\%$ and $81\% \leq APD_{rev}/APD_{max} \leq 84\%$). (b) Relationship between the $\Delta[Ca^{2+}]_i$ of the $(N+1)$st-beat versus the $\Delta[Ca^{2+}]_i$ of the (N)th-beat, also indicates that phase reversal in consecutive beats occurs when $\Delta[Ca^{2+}]_i$ falls within a small range of its minimum and maximum values ($214\% \leq \Delta[Ca^{2+}]_{i,rev}/\Delta[Ca^{2+}]_{i,min} \leq 232\%$, and $37\% \leq \Delta[Ca^{2+}]_{i,rev}/\Delta[Ca^{2+}]_{i,max} \leq 41\%$), as indicated by the red symbols. Where APD_{rev} is the APD value in which a phase reversal occurs, APD_{min} is the minimum APD value in the APD time series, APD_{max} is the maximum APD value in the APD time series, $\Delta[Ca^{2+}]_{i,rev}$ is the $\Delta[Ca^{2+}]_i$ value in which a phase reversal occurs, $\Delta[Ca^{2+}]_{i,min}$ is the minimum $\Delta[Ca^{2+}]_i$ value in the $\Delta[Ca^{2+}]_i$ time series, and $\Delta[Ca^{2+}]_{i,max}$ is the maximum $\Delta[Ca^{2+}]_i$ value in the $\Delta[Ca^{2+}]_i$ time series.

which is a subthreshold early after-depolarization (sEAD). This secondary Ca^{2+} release also results in a longer time for $[Ca^{2+}]_i$ to reach its peak value, and is seen only in beats associated with a large $[Ca^{2+}]_i$ that is on an every other beat basis [see Fig. 2(b)].

Significantly, in Fig. 2(b), after sustained concordant alternans [seen in Fig. 1(b)] between the $\Delta[Ca^{2+}]_i$ and APD in which a large/small (indicated as A/B) $\Delta[Ca^{2+}]_i$ corresponds to a long/short (indicated as A/B) APD, in *beat 3*, one observes that a phase reversal between $\Delta[Ca^{2+}]_i$ and APD occurs (i.e., a small $\Delta[Ca^{2+}]_i$ is associated with a long APD). It is likely that what causes the phase reversal between $[Ca^{2+}]_i$ and APD is the $\Delta[Ca^{2+}]_i$ amplitude, which in this beat is larger than the amplitude of the previous small $\Delta[Ca^{2+}]_i$, and is smaller than the previous large $\Delta[Ca^{2+}]_i$ [see Fig. 1(b), and also Fig. 3(a) and (b)]; $\Delta[Ca^{2+}]_i$ influences the balance of the depolarizing and repolarizing currents through the LTCC and NCX, and their effect on APD.

In *beat 4*, one observes that the $\Delta[Ca^{2+}]_i$ and APD continue to be out of phase, in which case, a large $\Delta[Ca^{2+}]_i$ coincides with a short APD. In *beats 5 and 6*, one sees that the $\Delta[Ca^{2+}]_i$ and APD are again in-phase, but because $\Delta[Ca^{2+}]_i$ is still within a critical range (see Fig. 3(a) and (b) later) between a small and a large $\Delta[Ca^{2+}]_i$ (i.e., of the first, eighth, ninth, and tenth beat), the APD can be either short or long, which is likely to result in a phase reversal between $\Delta[Ca^{2+}]_i$ and APD. Indeed, in *beat 7,* there is a phase reversal between $\Delta[Ca^{2+}]_i$ and APD, that is a large $\Delta[Ca^{2+}]_i$ (larger than that in beat 6), corresponds to a short APD.

Thereafter, in *beat 8,* phase reversal again results in in-phase alternans of $\Delta[Ca^{2+}]_i$ and APD, which is maintained in subsequent beats.

Since reduced SR Ca^{2+} uptake alone could lead to smaller Ca^{2+} release and $[Ca^{2+}]_i$, the beat-to-beat $\Delta[Ca^{2+}]_{SR}$ (defined as the diastolic minus the systolic $[Ca^{2+}]_{SR}$) oscillations have been quantified from the computer-generated data (using the same simultaneous AP- and $[Ca^{2+}]_i$-clamp approach). It was observed that $\Delta[Ca^{2+}]_{SR}$ alternated between beats corresponding to small and large $[Ca^{2+}]_i$ during alternans [see Fig. 2(c)]; however, $\Delta[Ca^{2+}]_{SR}$ was almost constant in beats corresponding to nonchanging $[Ca^{2+}]_i$.

B. Relationship of Beat-to-Beat $[Ca^{2+}]_i$ and APD During Alternans

Analysis of the beat-to-beat $\Delta[Ca^{2+}]_i$ and APD for the whole-data record revealed that discordant alternans occurred four times [red pixels in Fig. 3(a) and (b)]. Interestingly, similarly to the example presented in Fig. 1(b), all four phase transitions of concordant to discordant alternans were transient, which resulted into discordant alternans to be reverted back to sustained concordant alternans, within a few beats.

Fig. 3(a) demonstrates the relationship between the $\Delta[Ca^{2+}]_i$ and APD. One observes that phase reversal occurs for APD values that fall within $113\% \leq APD_{rev}/APD_{min} \leq 117\%$ and $81\% \leq APD_{rev}/APD_{max} \leq 84\%$, where APD_{rev} is the APD value in which a phase reversal occurs, and APD_{min}/APD_{max} are the minimum/maximum APD value, respectively, in the APD time series.

On the other hand, Fig. 3(b) which presents the relationship between the $\Delta[Ca^{2+}]_i$ of the $(N+1)$st-beat versus the $\Delta[Ca^{2+}]_i$ of the (N)th-beat, indicates that phase reversal occurs when $\Delta[Ca^{2+}]_i$ falls within a small range of its minimum and maximum values of the $\Delta[Ca^{2+}]_i$ time

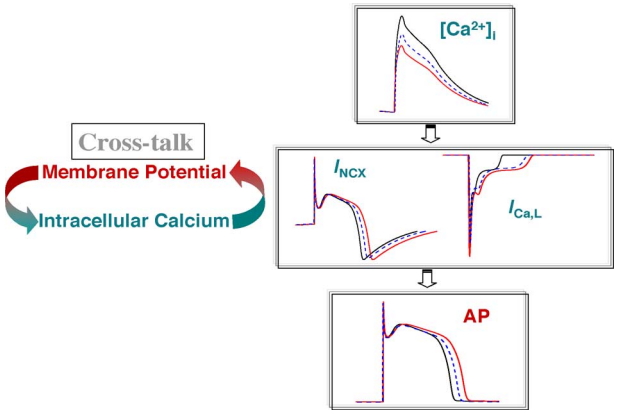

Fig. 4. Schematic of the apparent dependence of the shape of the AP waveform on the NCX that contributes either a depolarizing or repolarizing current during the AP and the LTCC that contributes a depolarizing current. Since both the NCX and LTCC are directly mediated by $[Ca^{2+}]_i$, a large calcium transient (in black) first causes the NCX to reverse earlier, thus contributing a smaller repolarizing current, and thus, contributing to AP prolongation, and second causes acceleration of the LTCC-Ca^{2+}-mediated inactivation that would cause AP shortening; one expects the opposite results for a small calcium transient (in red). Thus, the effect of $[Ca^{2+}]_i$ on the membrane potential is defined by the net balance of these two currents.

series ($214\% \leq \Delta[Ca^{2+}]_{i,\mathrm{rev}}/\Delta[Ca^{2+}]_{i,\mathrm{min}} \leq 232\%$ and $37\% \leq \Delta[Ca^{2+}]_{i,\mathrm{rev}}/\Delta[Ca^{2+}]_{i,\mathrm{max}} \leq 41\%$), as indicated by the red symbols; where $\Delta[Ca^{2+}]_{i,\mathrm{rev}}$ is the $\Delta[Ca^{2+}]_i$ value in which a phase reversal occurs, and $\Delta[Ca^{2+}]_{i,\mathrm{min}}/\Delta[Ca^{2+}]_{i,\mathrm{max}}$ are the minimum/maximum $\Delta[Ca^{2+}]_i$ values, respectively, in the $\Delta[Ca^{2+}]_i$ time series.

Thus, one sees that the $\Delta[Ca^{2+}]_i$ and APD oscillations change phase between each other, when $\Delta[Ca^{2+}]_i$ is within a critical range between a small and a large $\Delta[Ca^{2+}]_i$.

IV. Discussion

The present study presents the first report of discordant $[Ca^{2+}]_i$ and AP alternans in the cardiac myocyte, and attempts to explore the mechanisms underlying the discordant relationship between $[Ca^{2+}]_i$ and AP alternans.

The hybrid, experimental–computational approach used allowed the opening of the closed-loop system of the subcellular Ca^{2+} homeostatic mechanisms, and study their individual effect on the AP, without inadvertently perturbing the system under study. Specifically, it resulted in the following novel findings: 1) elevated SR Ca^{2+} results in aberrant SR Ca^{2+} release and in $[Ca^{2+}]_i$ alternans and 2) it established the presence of discordant alternans between the $[Ca^{2+}]_i$ and AP at the myocyte level, and the importance of $[Ca^{2+}]_i$ in defining the in- or out-of-phase relationship between $[Ca^{2+}]_i$ and AP.

The apparent inter-dependence of the shape of the AP waveform on the NCX which contributes either a depolarizing or repolarizing current during the AP, and the LTCC which contributes a depolarizing current, and their effect on $[Ca^{2+}]_i$ and AP alternans, is presented in Fig. 4. Since both the NCX and LTCC are directly mediated by $[Ca^{2+}]_i$, a large calcium transient (in black) first causes the NCX to reverse earlier, thus contributing a smaller repolarizing current, and thus, contributing to AP prolongation, and second causes acceleration of the LTCC Ca^{2+}-mediated inactivation that causes AP shortening; one expects the opposite results for a small calcium transient (in red). Thus, the effect of $[Ca^{2+}]_i$ on the membrane potential is defined by the net balance of these two currents.

Overall, the biophysical observations of this and previous studies [15] are consistent with experiments in heart cells [19], in planar lipid bilayers [20], and cardiac vesicles [21] that confirm that Ca^{2+} in the SR lumen influences RyR gating such that RyRs are more likely to be triggered by cytosolic Ca^{2+} *when* SR luminal Ca^{2+} is elevated, which increases spontaneous SR Ca^{2+} release [22] and the delayed after-depolarization (DAD) amplitude threshold to trigger an AP [23]. Furthermore, these findings agree with those of Diaz *et al.* [9] in which, during alternans, secondary releases and biphasic $[Ca^{2+}]_i$ were observed in tetracaine-treated myocytes. These secondary releases were attributed to the increased spatial and temporal desynchronization of SR Ca^{2+} release, during which, in a given region of a myocyte, SR Ca^{2+} release propagated as a wave, the amplitude of which could alternate on a beat-to-beat basis.

At the whole-heart level, optical mapping studies in normal hearts have shown that discordant AP alternans (reflecting two areas in the heart that oscillate with opposite phase) were associated with a state of marked cardiac electrical instability, since ventricular fibrillation was always preceded by discordant and never by concordant AP repolarization alternans [1], [14]. This pattern of inhomogeneity was consistently induced at a critical threshold heart rate, and was largely independent of the pacing site [1], suggesting that it was caused by heterogeneities of cellular repolarization properties rather than heterogeneous propagation delay. Interestingly, in this study, alternans most commonly involved the slope of the AP plateau and the onset of final repolarization.

In summary, SR Ca^{2+} overload that results in spontaneous SR Ca^{2+} release and stimulates additional Ca^{2+} extrusion via the NCX which in turn produces an inward, depolarizing current and sub-threshold triggered depolarizations, are the underlying events for $[Ca^{2+}]_i$ and AP alternans. Furthermore, the finding that the $[Ca^{2+}]_i$ and APD can oscillate in an uncorrelated manner is likely to constitute the ventricular myocyte as the smallest unit underlying cardiac alternans and increased susceptibility to arrhythmogenesis.

References

[1] K. R. Laurita, J. M. Pastore, and D. S. Rosenbaum, "How restitution, repolarization, and alternans form arrhythmogenic substrates: Insights from high-resolution optical mapping," in *Cardiac Electrophysiology: From Cell to Bedside*, D. P. Zipes and J. Jalife, Eds., 2nd ed. Philadelphia, PA: Saunders, 1999, pp. 239–248.

[2] A. A. Armoundas, G. F. Tomaselli, and H. D. Esperer, "Pathophysiological basis and clinical application of T-wave alternans," *JACC*, vol. 40, pp. 207–217, 2002.

[3] A. A. Armoundas, S. H. Hohnloser, T. Ikeda, and R. J. Cohen, "Can microvolt T-wave alternans testing reduce unnecessary defibrillator implantation?" *Nat. Clin. Pract. Cardiovasc. Med.*, vol. 2, pp. 522–528, 2005.

[4] A. Mahajan, D. Sato, Y. Shiferaw, A. Baher, L. H. Xie, R. Peralta, R. Olcese, A. Garfinkel, Z. Qu, and J. N. Weiss, "Modifying L-type calcium current kinetics: Consequences for cardiac excitation and arrhythmia dynamics," *Biophys. J.*, vol. 94, pp. 411–423, 2008.

[5] F. Hua, D. C. Johns, and R. F. Gilmour Jr., "Suppression of electrical alternans by overexpression of HERG in canine ventricular myocytes," *Amer. J. Physiol. Heart Circ. Physiol.*, vol. 286, pp. H2342–H2351, 2004.

[6] J. J. Fox, J. L. McHarg, and R. F. Gilmour, Jr., "Ionic mechanism of electrical alternans," *Amer. J. Physiol. Heart Circ. Physiol.*, vol. 282, pp. H516–H530, 2002.

[7] P. N. Jordan and D. J. Christini, "Action potential morphology influences intracellular calcium handling stability and the occurrence of alternans," *Biophys. J.*, vol. 90, pp. 672–680, 2006.

[8] J. I. Goldhaber, L. H. Xie, T. Duong, C. Motter, K. Khuu, and J. N. Weiss, "Action potential duration restitution and alternans in rabbit ventricular myocytes: The key role of intracellular calcium cycling," *Circ. Res.*, vol. 96, pp. 459–466, 2005.

[9] M. E. Diaz, D. A. Eisner, and S. C. O'Neill, "Depressed ryanodine receptor activity increases variability and duration of the systolic Ca2+ transient in rat ventricular myocytes," *Circ. Res.*, vol. 91, pp. 585–593, 2002.

[10] E. Chudin, J. Goldhaber, A. Garfinkel, J. Weiss, and B. Kogan, "Intracellular Ca(2+) dynamics and the stability of ventricular tachycardia," *Biophys. J.*, vol. 77, pp. 2930–2941, 1999.

[11] J. Kockskamper, A. V. Zima, and L. A. Blatter, "Modulation of sarcoplasmic reticulum Ca2+ release by glycolysis in cat atrial myocytes," *J. Physiol.*, vol. 564, pp. 697–714, 2005.

[12] J. Hüser, Y. G. Wang, K. A. Sheehan, F. Cifuentes, S. L. Lipsius, and L. A. Blatter, "Functional coupling between glycolysis and excitation–contraction coupling underlies alternans in cat heart cells," *J. Physiol. (Lond.)*, vol. 524, pp. 795–806, 2000.

[13] J. M. Pastore, S. D. Girouard, K. R. Laurita, F. G. Akar, and D. S. Rosenbaum, "Mechanism linking T-wave alternans to the genesis of cardiac fibrillation," *Circulation*, vol. 99, pp. 1385–1394, 1999.

[14] J. M. Pastore and D. S. Rosenbaum, "Role of structural barriers in the mechanism of alternans-induced reentry," *Circ. Res.*, vol. 87, pp. 1157–1163, 2000.

[15] A. A. Armoundas, "Mechanism of abnormal sarcoplasmic reticulum calcium release in canine left ventricular myocytes results in cellular alternans," *IEEE Trans. Biomed. Eng.*, vol. 56, no. 2, pp. 220–228, Feb. 2009.

[16] A. A. Armoundas, I. A. Hobai, G. F. Tomaselli, R. L. Winslow, and B. O'Rourke, "Role of sodium–calcium exchanger in modulating the action potential of ventricular myocytes from normal and failing hearts," *Circ. Res.*, vol. 93, pp. 46–53, 2003.

[17] R. L. Winslow, J. Rice, S. Jafri, E. Marban, and B. O'Rourke, "Mechanisms of altered excitation–contraction coupling in canine tachycardia-induced heart failure, II: Model studies," *Circ. Res.*, vol. 84, pp. 571–586, 1999.

[18] J. L. Greenstein, R. Wu, S. Po, G. F. Tomaselli, and R. L. Winslow, "Role of the calcium-independent transient outward current I(to1) in shaping action potential morphology and duration," *Circ. Res.*, vol. 87, pp. 1026–1033, 2000.

[19] Y. Li, E. G. Kranias, G. A. Mignery, and D. M. Bers, "Protein kinase A phosphorylation of the ryanodine receptor does not affect calcium sparks in mouse ventricular myocytes," *Circ. Res.*, vol. 90, pp. 309–316, 2002.

[20] I. Gyorke and S. Gyorke, "Regulation of the cardiac ryanodine receptor channel by luminal Ca^{2+} involves luminal Ca^{2+} sensing sites," *Biophys. J.*, vol. 75, pp. 2801–2810, 1998.

[21] N. Ikemoto, M. Ronjat, L. G. Meszaros, and M. Koshita, "Postulated role of calsequestrin in the regulation of calcium release from sarcoplasmic reticulum," *Biochemistry*, vol. 28, pp. 6764–6771, 1989.

[22] H. Satoh, L. A. Blatter, and D. M. Bers, "Effects of [Ca2+]i, SR Ca2+ load, and rest on Ca2 +spark frequency in ventricular myocytes," *Amer. J. Physiol.*, vol. 272, pp. H657–H668, 1997.

[23] C. H. Orchard, D. A. Eisner, and D. G. Allen, "Oscillations of intracellular Ca2+ in mammalian cardiac muscle," *Nature*, vol. 304, pp. 735–738, 1983.